ELSEVIER

Imaging Alzheimer's disease pathology: one target, many ligands

Andrew Lockhart

GlaxoSmithKline, Addenbrooke's Centre for Clinical Investigation (ACCI), Box No. 128, Addenbrookes Hospital, Hills Road, Cambridge CB2 2GG, UK

Over the past five years there has been a surge of interest in using positron emission tomography (PET) to determine the *in vivo* density of the senile plaque, a key pathological feature of Alzheimer's disease. The development of the tracers [^{11}C]-PIB, [^{11}C]-SB13 and [^{18}F]-FDDNP has coincided with drug strategies aimed at altering the brain metabolism of amyloid-β peptides. The evolution of these novel ligands serves not only as an excellent example of how rapidly imaging technologies can progress but also as a reminder that the fundamental biological knowledge, which is necessary to fully interpret the PET data, can be left trailing behind.

At their best, *in vivo* imaging modalities such as positron emission tomography (PET) and magnetic resonance imaging (MRI) have the ability to provide quantitative, high-resolution data that detail biological processes and structures, thus ensuring that these complementary imaging techniques have the ability to influence key decision points in the drug discovery process [1]. For example, with preclinical PET, biodistribution studies provide quantitative information on the penetration of the labelled drug into different tissue compartments, and receptor-occupancy studies can aid dose selection for future clinical trials. In the clinical setting, and especially in early-phase trials, the readouts from imaging techniques can be useful in enriching patient populations or acting as surrogate or direct markers for drug activity (i.e. pharmacodynamic markers). Imaging has the greatest potential to provide the greatest impact on neurodegenerative and psychiatric disease research owing to the present inability to non-invasively and routinely sample the brain.

Alzheimer's disease (AD), the most common form of dementia, slowly destroys cognitive regions of the brain. Despite advances in clinical screening since its first characterization a century ago [2], the method for the definitive diagnosis of AD is still neuropathological examination of the brain [3]. The gross pathology of the AD brain at postmortem is typically characterized by narrowing of the gyri and widening of the sulci, thinning of cortical ribbon, hippocampal atrophy and ventricular enlargement; however, none of these features are sufficient to define AD [4]. Instead, the key pathological features of AD – senile plaques (SPs) and neurofibrillary tangles (NFTs) – are identified using either histopathological dyes (e.g. Congo Red or thioflavin S) or immunohistochemistry. SPs and NFTs are mainly composed of aggregated (polymeric) forms of amyloid-β (Aβ) peptide (both 1–40 and 1–42) and hyperphosphorylated Tau (phospho-Tau) proteins, respectively. The presence of these lesions at sufficient densities with a defined neuroanatomy is considered diagnostic for AD [3]. In addition, characteristic AD pathology includes neuronal loss or atrophy, gliosis and, in many cases, the presence of cerebral amyloid angiopathy (CAA) and Lewy bodies (LBs) [5].

AD is primarily a disorder that affects aging individuals, with accompanying risk factors that are associated with an APOE4 genotype [6] and that overlap with those of cardiovascular disease [7]. Familial AD cases are rare, accounting for ~5% of total cases, and are linked to mutations either in the gene encoding Aβ peptides [e.g. the amyloid precursor protein (APP)] or genes linked with Aβ cleavage from APP (e.g. those encoding Presenilin 1 and Presenilin 2) [8]. These familial cases, in particular, have provided a persuasive argument for the amyloid hypothesis of AD, which places the Aβ peptide as the central, causative disease agent [9]. In response to this theory, a range of interventional strategies aimed at either reducing the production of Aβ peptides (i.e. use of γ- and β-secretase inhibitors [10]) or modulating their clearance (i.e. 'active' and 'passive' immunization [11]) from the brain are at various stages in the drug-development process. These treatments

Corresponding author: Lockhart, A. (andrew.2.lockhart@gsk.com)

1359-6446/06/$ - see front matter © 2006 Elsevier Ltd. All rights reserved. doi:10.1016/j.drudis.2006.10.008

will provide a crucial, and perhaps definitive, test of the importance of Aβ in disease onset and progression.

However, to progress these Aβ-modulating drugs into the clinic rapidly, reliable (and, perhaps less importantly, specific) markers of disease activity and progression are required. As with all neurological disorders, detecting peripheral (blood) markers is challenging because the blood–brain barrier prevents the free diffusion of potential analytes from the central nervous system compartment. Cerebrospinal fluid (CSF) provides a more attractive biofluid than plasma for marker identification because its composition is anatomically more reflective of the interstitial fluid that bathes the parenchymal cells. However, the necessity to collect CSF via lumbar puncture (in living individuals) means that there is still a considerable spatial factor (and a cellular barrier) between the fluid withdrawn by the needle and the neuronal cells. This is echoed in the observation that, at present, a CSF measure of soluble Aβ1–42 combined with a Tau:phospho-Tau ratio is the only specific clinical marker of AD [12,13].

The employment of an imaging modality that could track disease progression and, in addition, be sensitive to therapeutic intervention is extremely attractive. One such technology that has attracted extensive attention in the AD field is PET, which employs imaging agents (radiotracers) with high affinity for the aggregated forms of Aβ found in SPs. PET is a non-invasive imaging technique that enables *in vivo* quantification of biochemical and physiological processes [14]. Clearly, the low resolution of PET (compared with MRI) does not enable the visualization of individual SPs. Instead, regional maps (i.e. tomograms) that reflect areas of ligand retention, and hence plaque density, are constructed.

Out of the myriad of agents that have been reported to target Aβ polymers, only three have so far moved forward into evaluation studies using cohorts of AD patients: [^{18}F]-FDDNP [15], [^{11}C]-PIB [16] and [^{11}C]-SB13 [17] (full chemical nomenclature is provided in Box 1). The results from initial studies are encouraging; all three ligands display uptake and retention in areas of the brain that are known to contain high densities of plaques [18]. Here, I focus on: (i) the occurrence of amyloid structures in AD (and other neuropathologies); (ii) the chemical evolution of the amyloid imaging tracers; (iii) models of ligand binding to Aβ fibrils; (iv) *in vivo* imaging studies using amyloid imaging agents; and (v) the clinical relevance of amyloid in AD.

BOX 1

Chemical nomenclature of compounds relevant to this review

6-Me-BTA-1	2-[4′-(methylamino)phenyl]-6-methylbenzothiazole
BTA-1	2-[4′-(methylamino)phenyl]benzothiazole
6-OH-BTA-1 (PIB)	2-[4′-(methylamino)phenyl]-6-hydroxybenzothiazole (Pittsburgh compound B)
DDNP	1,1-dicyano-2-[6-(dimethylamino)naphthalene-2-yl]propene
FDDNP	2-(1-{6-[(2-fluoroethyl(methyl)amino]-2-naphthyl} ethylidene)malononitrile
FEM-IMPY	6-iodo-2-[4′-*N*-(2-fluoroethyl)methylamino] phenylimidazo[1,2-*a*]pyridine
SB13	4-*N*-methylamino-4′-hydroxystilbene
BSB	(trans,trans)-1-bromo-2,5-bis(3-hydroxycarbonyl-4-hydroxy)styrylbenzene
X34	1,4-bis(3-carboxy-4-hydroxyphenylethenyl)benzene
Methoxy-X04	1,4-bis(4′-hydroxystyryl)-2-methoxybenzene
FENE	1-{6-[(2-fluoroethyl)(methyl)amino]naphthalen-2-yl}ethone
TZPI	2-[4′-(4″-methylpiperazin-1-yl)phenyl]-6-iodobenzothiazole

The occurrence of amyloid structures in AD

Fundamental to the understanding of the *in vivo* signal generated by any PET tracer is a detailed knowledge of the receptor complex to which the ligand binds. In the case of AD, the 'receptor' is a polymer composed of Aβ peptide subunits that are arranged in an ordered, hierarchical manner into a mature structure termed an amyloid fibril [19]. The polypeptide backbone of each Aβ peptide in the fibril is folded into the same basic motif, termed a β-pleated sheet or a cross β-structure [20]. It is the unique stereochemistry of this fold that confers the ability of the fibrils to bind specifically to the histological dyes Congo Red and thioflavins S and T [19]. These stains are important because they serve as initial starting templates for two of the chemical series developed as potential Aβ PET ligands (see later section about the chemical evolution of the amyloid imaging tracers).

Within the AD brain there are two topologically distinct extracellular pools of fibrils composed of Aβ peptides: (i) parenchymal SPs; and (ii) deposits in the walls of arteries and arterioles of the cerebral cortex (and the leptomeninges) that give rise to cerebrovascular amyloid angiopathy (CAA) [21] (Table 1). There are also distinct biochemical differences between these two Aβ pools. SPs usually have high concentrations of Aβ1–42 species and, in addition, contain a number of post-translational modifications including oxidation, isomerizations and N-terminal truncations [22,23]. Vascular Aβ deposits are, by comparison, spared from post-translational modification [24] and tend to contain high concentrations of Aβ1–40 peptides [25,26]. Understanding the relative tracer-binding characteristics of these two amyloid pools *in vivo* is fundamental to

TABLE 1

Summary of amyloid pathologies in AD, tauopathies (TauP) and Lewy body dementias (LBD)

Pathological feature	Polypeptide	Disease[a]			Amyloid location	Post-translational modifications
		AD	TauP	LBD		
Senile plaques	Aβ peptides 1–40	+	–	(+)	Extracellular	+ (truncation, racemization or oxidation)
Cerebral amyloid angiopathy	and 1–42	(+)	(+)	(+)	Abluminal[b]	–
Neurofibrillary tangles	Tau	+	+	(+)	Intraneuronal	+ (phosphorylation or truncation)
Lewy bodies	α-Synuclein	(+)	(+)	+	Intraneuronal	+ (phosphorylation)

[a] +, pathology always present; (+), variable pathology; –, no pathology.
[b] in cerebral blood vessels.

interpreting tracer retention accurately because the fibrillar Aβ associated with CAA appears to be resistant to immune-mediated clearance mechanisms [11]. Aβ peptides can also be deposited in the parenchyma as diffuse plaques. The role of these plaques in the pathogenesis of AD is unclear and their presence in large numbers has been reported in aged, cognitively normal individuals [8]. However, this aggregated form does not contain large amounts of β-pleated sheet (i.e. it is non-fibrillar) and, hence, is only reported to weakly bind dyes such as Congo Red and the thioflavins [27,28]. The interaction of the PET tracers with this pool of amyloid, which is associated with diffuse plaques, is, therefore, expected to be low, although this has not been formally demonstrated.

The occurrence of amyloid structures in other neuropathologies

A wide range of proteins or protein fragments share the ability to form amyloid and, although the constituent polypeptides do not seem to share any obvious sequence homology, they all acquire the same basic protein fold (the β-pleated sheet) when formed into a fibrillar structure [20]. Two such relevant polypeptides for AD are the hyperphosphorylated Tau isoforms and α-synuclein, which form the fibrillar constituents of NFTs and LBs, respectively (Table 1). The importance of the interaction between the amyloid tracers and these intraneuronal deposits is, at present, unknown because these pools of amyloid have not been studied in any detail (see later section on models of ligand binding to Aβ fibrils).

In addition to AD, several neurological disorders are also associated with the deposition of amyloid fibrils, including the LB diseases (e.g. dementia with LBs and Parkinson's disease), tauopathies (e.g. frontotemporal dementia, Pick's disease and progressive supranuclear palsy), the polyglutamine (polyQ) expansion diseases (e.g. Huntington's disease, Kennedy's disease and spinocerebellar ataxia), the spongiform encephalopathies (e.g. Creutzfeldt-Jacob disease) and familial amyotrophic lateral sclerosis [29]. A fuller understanding of the amyloid specificity of the tracers might also enable their application in a wider range of diseases.

The chemical evolution of the Aβ-imaging tracers

The first attempts to develop an amyloid probe were based around a series of Congo Red derivatives with only modest binding affinities (μM) for Aβ peptide fibrils [30,31]. These early studies recognized the importance of improving the brain penetrance of the dye for neuroimaging, and a further study demonstrated that amyloid specificity was feasible by manipulating the stereochemistry of the ligand [32]. Currently, there are three broad chemotype classes of ligands that are derived from either the histological dyes thioflavin T and Congo Red or the novel hydrophobic dye DDNP (Figure 1).

Derivatization of these dyes has led to a multitude of new ligands that, especially for the histochemical dyes, have high hydrophobicity owing to the removal of their charged moieties. This work has also enabled compatibility of these novel ligands with the rapid synthetic chemistry routes required to incorporate the short-lived positron-emitting radionuclides (Figure 2). To date, compounds derived from Congo Red (e.g. BSB [33], X34 [34] and X04 [35]; Figure 2) display poor brain uptake, limiting their potential use as PET ligands, although their strong fluorescent properties have found applications in optical imaging techniques [36,37]. The hydroxystilbene SB13 [38], although classified as a Congo Red derivative in Figure 2, could be considered stereochemically analogous to PIB owing to the respective positioning of the *N*-methyl aminophenyl and hydroxyl groups.

The transition of a ligand from bench to bedside usually follows the same workflow pattern: (i) *in vitro* screening using Aβ fibrils to derive K_d or K_i values; (ii) *ex vivo* autoradiography using a

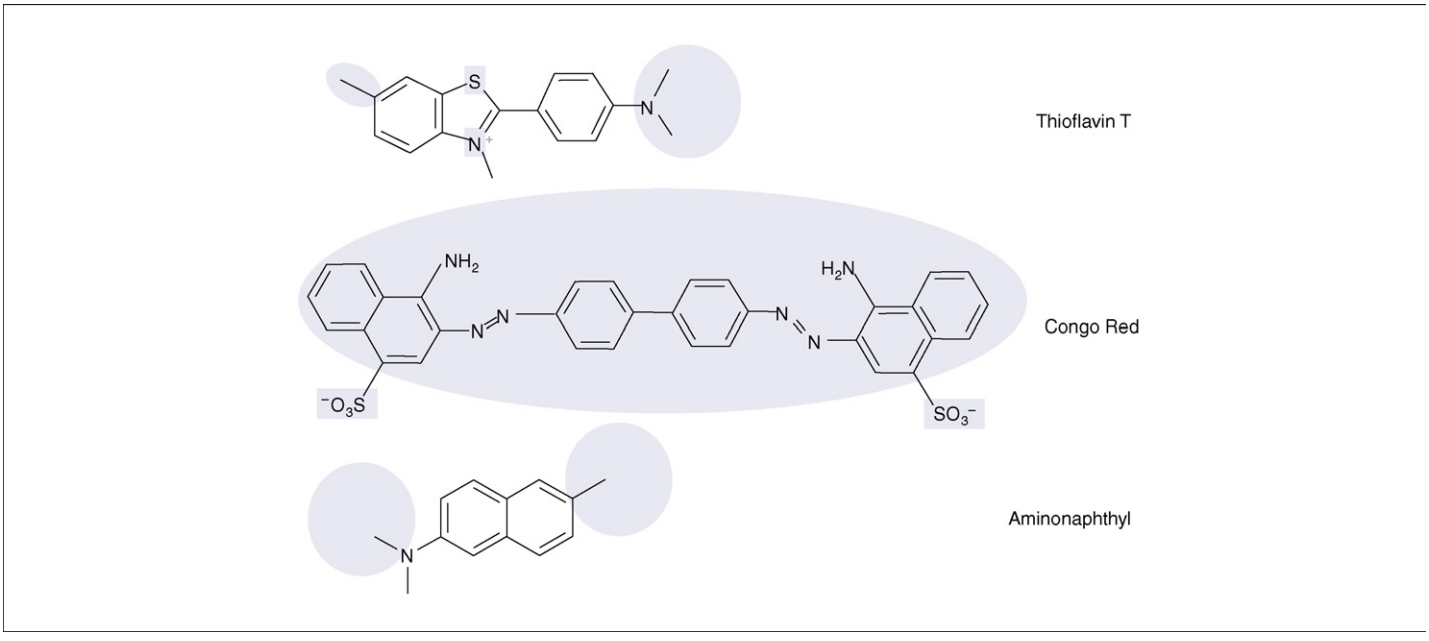

FIGURE 1

Starting pharmacophores for imaging-agent development. Shaded areas highlight major sites of derivatization that were aimed largely at removing charged groups and altering the hydrophobicity of the ligands. Of the three dyes, Congo Red displayed the greatest structural modification with the removal of the azo (N═N) bonds and the biphenyl rings. These changes lowered the molecular weight of the Congo Red backbone structure to a value compatible with good brain uptake.

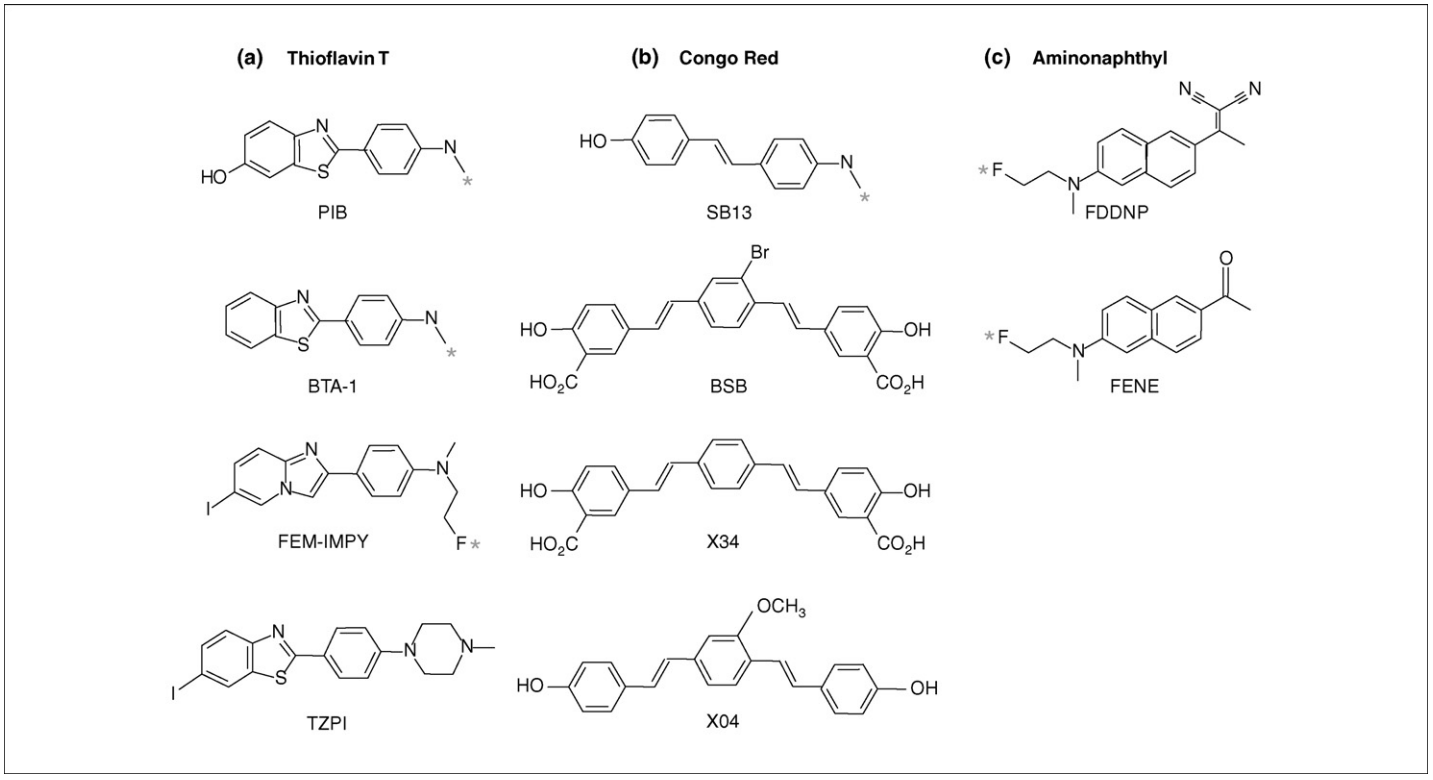

FIGURE 2

Selected amyloid-imaging agents to demonstrate structural divergence from starting pharmacophores. (a) Thioflavin T, **(b)** Congo Red and **(c)** aminonaphthyl were the starting pharmacophores. Structures for (a–c) are shown in Figure 1. * indicates the site of radionuclide labelling. Of the compounds shown, only BSB and X34 have retained their charged moieties (carboxylic acid groups), which are believed to limit their brain uptake and application in PET imaging studies.

positron-emitting radiolabelled version of the ligand with AD-brain sections or with brain sections from a transgenic mouse model of AD; (iii) a biodistribution study in a small animal (or occasionally a non-human primate); and, for a few ligands, (iv) deployment in patient cohorts.

One of the strange quirks preventing the smooth translation of these tracers into clinical imaging studies is that only a marginal retention of the radiotracers has been observed using transgenic models of AD [39,40]. This is despite the massive Aβ plaque load that can be detected in these animals using *in vivo* optical-imaging techniques such as two-photon microscopy [34] and *ex vivo* binding techniques [40]. Whatever the reasons for this inability to image the amyloid load using PET in transgenic mice, these findings remove a valuable screening tool for tracer development and the ability to translate imaging techniques directly from preclinical to clinical evaluation of Aβ modulating strategies.

Models of ligand binding to Aβ fibrils

The initial *in vitro* evaluations of members from each of the three chemotype classes (thioflavin T, Congo Red and DDNP) relied heavily on radioligand assays that use narrow ranges of ligand concentrations to derive binding constants (K_d and/or K_i values) and binding-site densities (B_{max} values). These studies indicated that, for each chemotype class, there was a high-affinity, independent (i.e. spatially distinct) binding site, and that these sites were present at low densities along the Aβ fibrils (with values of one tracer binding site per 400–2000 Aβ-peptide monomers [41,42]). However, more-detailed studies using a wider range of assay formats and conditions led to a radically different binding-site model by demonstrating that there were at least two additional classes of sites for the thioflavin T ligands and that these sites could bind Congo Red and DDNP derivatives [43,44]. Although the *in vivo* relevance of these additional ligand-binding sites is at present unclear, their occurrence provides additional potential targets for tracer development.

An approximate rule for predicting the success of a radiotracer is the ratio of B_{max}:K_d ratio, which is termed the binding potential (BP) [45]. As an example, the reported B_{max} and K_d values for [3H]-PIB binding to *in vitro* generated Aβ fibrils were 0.54 nM and 4.7 nM, respectively, producing a BP of 0.11 [46]. BPs greater than ten are usually associated with successful tracers, although there are examples of ligands used in imaging studies with considerably lower values [46]. Thus, in contrast to the initial imaging study [16], the [^{11}C]-labelled benzothiazole (BTA) derivatives were not predicted to elicit strong binding signals. This disparity was, in part, answered by the measurement of substantially higher B_{max} values for [3H]-PIB in homogenates derived from postmortem AD frontal-cortex specimens [47] and the further demonstration of a positive correlation between the levels of [3H]-PIB binding and the concentration of insoluble Aβ peptide in AD-brain homogenates [40].

These latter studies [41–43,46,47] question whether *in vitro* fibrillar structures that are representative of those found within SPs can be assembled accurately. The different classes of sites present on the *in vitro* assembled fibrils could reflect subtle conformational variants to those found within the SP [40,43]. However, this perhaps raises more questions and uncertainties regarding the physical and temporal factors required to induce enough

high-affinity binding sites to produce a sufficient binding signal *in vivo*. Perhaps the many post-translational modifications associated with the Aβ peptides isolated from SPs [22,23], and/or the many accessory proteins trapped within the plaques, have a role in controlling this process [48] (Table 1). Furthermore, if a therapeutic intervention induces a conformational change in the fibrillar structure, either through direct antibody binding (and subsequent complement activation and deposition) or by the partial removal of Aβ peptides from the polymers, it might be enough to cause a significant loss in signal that would not necessarily reflect a linear reduction in peptide levels. In addition, neuropathological data from the Aβ active immunization study indicated that, although SP-associated Aβ can be effectively removed from the brain parenchyma, the pool of fibrillar Aβ associated with CAA seems to be resistant to the vaccination protocol [49]. As noted, it will be important to understand the relative contribution that each of these spatially and biochemically distinct amyloid pools has on the retention of the tracers.

To date, no studies have quantitatively and systematically addressed the abilities of the tracers to bind to other forms of relevant neuropathological features such as NFTs and LBs. For example, the negative interaction of the BTA-1 derivatives with NFTs was investigated qualitatively with a combination of fluorescence microscopy and brain-homogenate-binding assays using a single concentration of [3H]-BTA-1 [46]. In addition, the reported interaction of FDDNP with SPs and NFTs were based on fluorescent microscopy studies that used much higher concentrations of the ligand than would be obtained in PET scans [42,50]. Further studies are clearly warranted in this area, both to provide confidence in tracer specificity and, as noted, to tease out their potential use in other neurological diseases associated with widespread amyloid deposition.

In vivo imaging studies using Aβ-imaging agents

The first of the Aβ-imaging agents to be deployed in a clinical setting was [^{18}F]-FDDNP [15], closely followed by [^{11}C]-PIB [16] and, more recently, by [^{11}C]-SB13 [17]. These clinical studies were all cross-sectional in nature and designed to be 'proof-of-concept', involving few subjects. All three tracers displayed increased retention in the AD-patient populations, however as noted later, the magnitude and the regional distribution of the binding signal obtained with [^{18}F]-FDDNP shows extensive variations when compared with the other ligands. At present, the tracer with the most supporting *in vivo* data is [^{11}C]-PIB.

The FDDNP study employed nine AD patients and seven age-matched control subjects [15]. MRI was used to predefine a series of regions of interest (ROIs) that included the pons, which was used as a reference tissue (i.e. a region with low ligand retention). Tracer retention, termed the relative retention time (RRT), within a ROI was calculated using data collected 12–125 min post-injection, and expressed relative to the pons; a higher RRT was equated with an increased density of amyloid deposits. The highest RRT values for [^{18}F]-FDDNP were associated with the ROI containing the hippocampus, amygdala and entorhinal cortex. Increased ligand retention was also associated with frontal, parietal, temporal (medial) and occipital lobes in AD. However, the specific signal from this tracer was only ~0.3-fold that of the reference tissue in the regions of highest retention, which contrasts with ~1.5–2.0-fold specific signal, with respect to the reference tissue, associated with the [^{11}C]-PIB [16] and [^{11}C]-SB13 tracers [17].

The FDDNP study is additionally interesting for two reasons. First, the authors did not attempt to define the derived *in vivo* signal as being either SP- or NFT-specific but, instead, relied on their preclinical data, which demonstrated a binding component to each of these pathological features, to provide additional evidence that the pattern of ligand retention was consistent with their probe imaging both amyloid structures [42,50]. The observation that the highest RRT value was associated with the hippocampus, amygdala and entorhinal cortex is potentially consistent with a strong Tau component in the binding signal because these areas are associated with high levels of NFT deposition [51]. The comparatively lower signal associated with the frontal cortical areas, where a higher SP load would be expected, might also suggest more specificity towards tangle pathology. Consistent with this, recent *in vitro* data challenge the finding that there are two high-affinity (low nM) sites for FDDNP on Aβ fibrils [42] by providing evidence that the ligand binds with only a moderate affinity (~300 nM) to a single site on the polymer [44]. Second, using the hippocampus, amygdala and entorhinal cortex RRT values, a correlation between higher ligand retention and lower cognitive status (measured using a range of neuropsychological tests) was demonstrated [15]. Together, these observations could corroborate studies demonstrating that tangle density provides a sensitive index of cognitive decline [51].

The first clinical application using [^{11}C]-PIB was performed with a cohort of 16 patients with mild AD and nine age-matched, non-demented controls [16]. The data from this study were presented as a semiquantitative standardized uptake variable (SUV) and demonstrated significant regional retention of ligand in areas of brain known to contain extensive SP deposits, with the highest uptake observed in the frontal cortex (approximately twofold higher than controls). Additional cortical areas displaying a significant uptake were the parietal, occipital and temporal regions. None of these areas were associated with significant retention of the tracer in the control population.

Subsequently, the semiquantitative nature of the initial PIB study was addressed through the use of arterial sampling to provide a fuller kinetic model, and MRI–PET co-registration (i.e. aligning PET images with MRI images) enabled partial volume corrections and the definition of ROIs [52]. The techniques used provided a stepping-stone to simplified methods of analysis by demonstrating that [^{11}C]-PIB PET data could be fully quantified and modelled. Tracer retention in the MRI-defined ROIs was expressed, normalized to a reference tissue (the cerebellum), in the form of distribution volume ratios (DVRs). Reassuringly, the regional distribution of the tracer in the AD patients was similar to that reported in the initial PIB study [16] and, again, the controls displayed low ligand retention.

In addition to the five AD patients and five controls, five mild cognitively impaired (MCI) subjects were also included. The importance of this group is that MCI is believed to represent a prodomal phase of AD, although a large proportion of this population (~50%) remains stable or returns to a normal phenotype [53]. Identifying those subjects at risk of disease progression (to AD) is, therefore, important because they could benefit most from treatment. The pattern of retention of [^{11}C]-PIB by the MCIs was

defined as either AD-like or control-like, with no apparent intermediate phenotype. Despite the small size of the study, this observation could be extremely important because it suggests that, in a subpopulation of MCI subjects, there is a plaque load comparable with that found in full-blown AD. A further study using [^{11}C]-PIB demonstrated an apparent inverse relationship between tracer retention and CSF Aβ1–42 levels in a mixed cohort of control, MCI and AD subjects [54]. Subjects with positive PIB-binding data were associated with a low CSF level of the peptide. However, this is not a linear relationship because subjects were associated with either one of two phenotypes: positive PIB-retention (low) Aβ1–42 levels; or negative PIB-retention (high) Aβ1–42 levels. No intermediate phenotypes were observed and, taken together with the earlier study [52], these observations suggest that plaque deposition is an early event in AD pathogenesis. It is important that these findings are followed up in larger cohorts and also through longitudinal tracking of disease progression from MCI to AD.

The [^{11}C]-SB13 study was not only testing the ability of the tracer to image SPs but also performed comparative scans using [^{11}C]-PIB in AD ($n = 5$) and control ($n = 6$) cohorts [17]. For both tracers, ROIs were defined by hand and the data analyzed from summed frames collected over the 120-min scan time. No arterial data were collected and, instead, the input function was derived from venous-plasma tracer levels. This led to differences in the data-analysis methods used in the two studies, see Refs [17,52], making direct comparison of these studies difficult. However, in the SB13 study [17], both tracers showed a similar pattern of selective higher uptake and retention, enabling a clear differentiation between the AD and control cases. ROIs found to be discriminatory for AD versus controls with [^{11}C]-SB13 were the striatum and the frontal occipital cortex. The data from [^{11}C]-PIB scans were similar but additionally found the temporal cortex to be discriminating. The fact that these two ligands produce comparable ligand-retention patterns is not surprising considering their structural similarities. Further differentiation of these ligands might only become apparent in studies using larger cohorts and additional patient phenotypes (such as MCIs and other dementias).

The clinical relevance of amyloids in AD

Although the presence of SPs and NFTs is considered diagnostic of AD, their precise role in disease precipitation and progression is less clear and has been a subject of contention [55]. In particular, this has been the case with respect to the role of SPs in disease progression, usually with stronger associations with NFT density and distribution [56,57]. Without wishing to enter further into this debate, it is clear that PET imaging now provides our first opportunity to obtain a temporal, global image of the brain during the AD process and, thus, we should not be surprised that the findings from PET studies deviate from the previous cross-sectional, postmortem studies. The key factor in understanding the imaging data is ensuring that the radiotracers themselves have a clearly defined binding profile.

Concluding remarks

The results of the initial *in vivo* imaging studies using [^{11}C]-PIB, [^{18}F]-FDDNP and [^{11}C]-SB13 in AD patient cohorts are encouraging because they broadly demonstrate retention of the probes in areas of the brain associated with SP deposition. Although these data provide a rationale for deploying the tracers as potential markers of amyloid-modulating drug activity, several factors still need to be addressed. First, the stability of the binding signal over the short time frame (compared with the underlying disease process) of early-phase clinical trials should be monitored. This is also linked with demonstrating a robust correlation between SP load and the measured *in vivo* binding signal. Second, the biological specificity, although strongly inferred from both *in vitro* and *ex vivo* binding studies, has not been demonstrated *in vivo* using receptor-blocking techniques. Although this approach could be technically challenging because of the potentially high density of ligand binding sites, this issue still needs to be tackled.

In summary, it is clear that we are now at an exciting point in the evolution of the amyloid tracers because they provide our first opportunity to monitor longitudinally the development and progression of a central pathological feature of AD. The ongoing readouts from studies using [^{11}C]-PIB, [^{18}F]-FDDNP and [^{11}C]-SB13 will provide additional confidence in deploying these tracers in clinical studies.

Acknowledgements

Thanks to J.R. Lamb and E.A. Rabiner for helpful discussions, and to J.L. Morgenstern for help with preparing the manuscript.

References

1 Garcia-Alloza, M. and Bacskai, B.J. (2004) Techniques for brain imaging *in vivo*. *Neuromolecular Med.* 6, 65–78
2 Alzheimer, A. (1907) Über eine eigenartige Erkrankung der Hirnrinde. *Allgemeine Zeitschrift für Psychiatrie und phychish-Gerichtliche Medizin (Berlin)* 64, 146–148
3 Mirra, S.S. *et al.* (1991) The Consortium to Establish a Registry for Alzheimer's Disease (CERAD). Part II. Standardization of the neuropathologic assessment of Alzheimer's disease. *Neurology* 41, 479–486
4 Mirra, S.S. *et al.* (1993) Making the diagnosis of Alzheimer's disease. A primer for practicing pathologists. *Arch. Pathol. Lab. Med.* 117, 132–144
5 Dekosky, S.T. (2001) Epidemiology and pathophysiology of Alzheimer's disease. *Clin. Cornerstone* 3, 15–26
6 Roses, A.D. (1996) Apolipoprotein E in neurology. *Curr. Opin. Neurol.* 9, 265–270
7 Keller, J.N. (2006) Age-related neuropathology, cognitive decline, and Alzheimer's disease. *Ageing Res. Rev.* 5, 1–13
8 Selkoe, D.J. and Schenk, D. (2003) Alzheimer's disease: molecular understanding predicts amyloid-based therapeutics. *Annu. Rev. Pharmacol. Toxicol.* 43, 545–584
9 Hardy, J. and Selkoe, D.J. (2002) The amyloid hypothesis of Alzheimer's disease: progress and problems on the road to therapeutics. *Science* 297, 353–356
10 Pangalos, M.N. *et al.* (2005) Disease modifying strategies for the treatment of Alzheimer's disease targeted at modulating levels of the β-amyloid peptide. *Biochem. Soc. Trans.* 33, 553–558
11 Boche, D. *et al.* (2006) Immunotherapy for Alzheimer's disease and other dementias. *Clin. Neuropharmacol.* 29, 22–27
12 Wallin, A.K. *et al.* (2006) CSF biomarkers for Alzheimer's disease: levels of β-amyloid, tau, phosphorylated tau relate to clinical symptoms and survival. *Dement. Geriatr. Cogn. Disord.* 21, 131–138
13 Hansson, O. *et al.* (2006) Association between CSF biomarkers and incipient Alzheimer's disease in patients with mild cognitive impairment: a follow-up study. *Lancet Neurol.* 5, 228–234
14 Wang, J. and Maurer, L. (2005) Positron emission tomography: applications in drug discovery and drug development. *Curr. Top. Med. Chem.* 5, 1053–1075

15 Shoghi-Jadid, K. *et al.* (2002) Localization of neurofibrillary tangles and β-amyloid plaques in the brains of living patients with Alzheimer disease. *Am. J. Geriatr. Psychiatry* 10, 24–35
16 Klunk, W.E. *et al.* (2004) Imaging brain amyloid in Alzheimer's disease with Pittsburgh Compound-B. *Ann. Neurol.* 55, 306–319
17 Verhoeff, N.P. *et al.* (2004) *In-vivo* imaging of Alzheimer disease β-amyloid with [11C]SB-13 PET. *Am. J. Geriatr. Psychiatry* 12, 584–595
18 Nordberg, A. (2004) PET imaging of amyloid in Alzheimer's disease. *Lancet Neurol.* 3, 519–527
19 Makin, O.S. and Serpell, L.C. (2002) Examining the structure of the mature amyloid fibril. *Biochem. Soc. Trans.* 30, 521–525
20 Makin, O.S. and Serpell, L.C. (2005) Structures for amyloid fibrils. *FEBS J.* 272, 5950–5961
21 Weller, R.O. and Nicoll, J.A. (2005) Cerebral amyloid angiopathy: both viper and maggot in the brain. *Ann. Neurol.* 58, 348–350
22 Kuo, Y.M. *et al.* (1997) Isolation, chemical characterization, and quantitation of Aβ 3-pyroglutamyl peptide from neuritic plaques and vascular amyloid deposits. *Biochem. Biophys. Res. Commun.* 237, 188–191
23 Kuo, Y.M. *et al.* (1998) Irreversible dimerization/tetramerization and post-translational modifications inhibit proteolytic degradation of Aβ peptides of Alzheimer's disease. *Biochim. Biophys. Acta* 1406, 291–298
24 Roher, A.E. *et al.* (1993) β-Amyloid-(1-42) is a major component of cerebrovascular amyloid deposits: implications for the pathology of Alzheimer disease. *Proc. Natl. Acad. Sci. U. S. A.* 90, 10836–10840
25 Attems, J. (2005) Sporadic cerebral amyloid angiopathy: pathology, clinical implications, and possible pathomechanisms. *Acta Neuropathol. (Berl.)* 110, 345–359
26 Tian, J. *et al.* (2006) Relationships in Alzheimer's disease between the extent of Aβ deposition in cerebral blood vessel walls, as cerebral amyloid angiopathy, and the amount of cerebrovascular smooth muscle cells and collagen. *Neuropathol. Appl. Neurobiol.* 32, 332–340
27 Braak, H. *et al.* (1989) Alzheimer's disease: mismatch between amyloid plaques and neuritic plaques. *Neurosci. Lett.* 103, 24–28
28 Mott, R.T. and Hulette, C.M. (2005) Neuropathology of Alzheimer's disease. *Neuroimaging Clin. N. Am.* 15, 755–765
29 Taylor, J.P. *et al.* (2002) Toxic proteins in neurodegenerative disease. *Science* 296, 1991–1995
30 Klunk, W.E. *et al.* (1994) Development of small molecule probes for the β-amyloid protein of Alzheimer's disease. *Neurobiol. Aging* 15, 691–698
31 Klunk, W.E. *et al.* (1995) Chrysamine-G binding to Alzheimer and control brain: autopsy study of a new amyloid probe. *Neurobiol. Aging* 16, 541–548
32 Ashburn, T.T. *et al.* (1996) Amyloid probes based on Congo Red distinguish between fibrils comprising different peptides. *Chem. Biol.* 3, 351–358
33 Lee, C.W. *et al.* (2001) Isomerization of (Z,Z) to (E,E)1-bromo-2, 5-bis-(3-hydroxycarbonyl-4-hydroxy)styrylbenzene in strong base: probes for amyloid plaques in the brain. *J. Med. Chem.* 44, 2270–2275
34 Styren, S.D. *et al.* (2000) X-34, a fluorescent derivative of Congo Red: a novel histochemical stain for Alzheimer's disease pathology. *J. Histochem. Cytochem.* 48, 1223–1232
35 Klunk, W.E. *et al.* (2002) Imaging Aβ plaques in living transgenic mice with multiphoton microscopy and methoxy-X04, a systemically administered Congo Red derivative. *J. Neuropathol. Exp. Neurol.* 61, 797–805
36 Skovronsky, D.M. *et al.* (2000) *In vivo* detection of amyloid plaques in a mouse model of Alzheimer's disease. *Proc. Natl. Acad. Sci. U. S. A.* 97, 7609–7614
37 Robbins, E.M. *et al.* (2006) Kinetics of cerebral amyloid angiopathy progression in a transgenic mouse model of Alzheimer disease. *J. Neurosci.* 26, 365–371
38 Ono, M. *et al.* (2003) 11C-labeled stilbene derivatives as Aβ-aggregate-specific PET imaging agents for Alzheimer's disease. *Nucl. Med. Biol.* 30, 565–571
39 Toyama, H. *et al.* (2005) PET imaging of brain with the β-amyloid probe, [11C]6-OH-BTA-1, in a transgenic mouse model of Alzheimer's disease. *Eur. J. Nucl. Med. Mol. Imaging* 32, 593–600
40 Klunk, W.E. *et al.* (2005) Binding of the positron emission tomography tracer Pittsburgh compound-B reflects the amount of amyloid-β in Alzheimer's disease brain but not in transgenic mouse brain. *J. Neurosci.* 25, 10598–10606
41 Zhuang, Z.P. *et al.* (2001) Radioiodinated styrylbenzenes and thioflavins as probes for amyloid aggregates. *J. Med. Chem.* 44, 1905–1914
42 Agdeppa, E.D. *et al.* (2001) Binding characteristics of radiofluorinated 6-dialkylamino-2-naphthylethylidene derivatives as positron emission tomography imaging probes for β-amyloid plaques in Alzheimer's disease. *J. Neurosci.* 21, RC189
43 Lockhart, A. *et al.* (2004) Evidence for the presence of three distinct binding sites for the thioflavin T class of alzheimer's disease PET imaging agents on β-amyloid peptide fibrils. *J. Biol. Chem.* 280, 7677–7684
44 Ye, L. *et al.* (2005) Delineation of positron emission tomography imaging agent binding sites on β-amyloid peptide fibrils. *J. Biol. Chem.* 280, 23599–23604
45 Mintun, M.A. *et al.* (1984) A quantitative model for the *in vivo* assessment of drug binding sites with positron emission tomography. *Ann. Neurol.* 15, 217–227
46 Mathis, C.A. *et al.* (2003) Synthesis and evaluation of 11C-labeled 6-substituted 2-arylybenzothiazoles as amyloid imaging agents. *J. Med. Chem.* 46, 2740–2754
47 Klunk, W.E. *et al.* (2003) The binding of 2-(4′-methylaminophenyl)benzothiazole to postmortem brain homogenates is dominated by the amyloid component. *J. Neurosci.* 23, 2086–2092
48 Liao, L. *et al.* (2004) Proteomic characterization of postmortem amyloid plaques isolated by laser capture microdissection. *J. Biol. Chem.* 279, 37061–37068
49 Nicoll, J.A. *et al.* (2003) Neuropathology of human Alzheimer disease after immunization with amyloid-β peptide: a case report. *Nat. Med.* 9, 448–452
50 Agdeppa, E.D. *et al.* (2003) *In vitro* detection of (S)-naproxen and ibuprofen binding to plaques in the Alzheimer's brain using the positron emission tomography molecular imaging probe 2-(1-[6-[(2-[(18)F]fluoroethyl)(methyl)amino]-2-naphthyl]ethylidene)malono nitrile. *Neuroscience* 117, 723–773
51 Braak, H. and Braak, E. (1995) Staging of Alzheimer's disease-related neurofibrillary changes. *Neurobiol. Aging* 16, 271–278
52 Price, J.C. *et al.* (2005) Kinetic modeling of amyloid binding in humans using PET imaging and Pittsburgh Compound-B. *J. Cereb. Blood Flow Metab.* 25, 1528–1547
53 Bruscoli, M. and Lovestone, S. (2004) Is MCI really just early dementia? A systematic review of conversion studies *Int. Psychogeriatr.* 16, 129–140
54 Fagan, A.M. *et al.* (2006) Inverse relation between *in vivo* amyloid imaging load and cerebrospinal fluid Aβ42 in humans. *Ann. Neurol.* 59, 512–519
55 Castellani, R.J. *et al.* (2006) Neuropathology of Alzheimer disease: pathognomonic but not pathogenic. *Acta Neuropathol. (Berl.)* 111, 503–509
56 Braak, H. and Braak, E. (1991) Neuropathological stageing of Alzheimer-related changes. *Acta Neuropathol. (Berl.)* 82, 239–259
57 Braak, E. *et al.* (1999) Neuropathology of Alzheimer's disease: what is new since A. Alzheimer? *Eur. Arch. Psychiatry Clin. Neurosci.* 249, 14–22

Reproduction of material from Elsevier articles

Interested in reproducing part or all of an article published by Elsevier, or one of our article figures? If so, please contact our *Global Rights Department* with details of how and where the requested material will be used. To submit a permission request online, please contact:

Elsevier
Global Rights Department
PO Box 800
Oxford OX5 1DX, UK
Phone: +44 (0)1865 843 830
Fax: +44 (0)1865 853 333
permissions@elsevier.com

Alternatively, please visit:

www.elsevier.com/locate/permissions